Electrical properties of stacking electrodes for flexible crystalline semiconductor photonic devices

2011 Semicond. Sci. Technol. 26 095018

(http://iopscience.iop.org/0268-1242/26/9/095018)

Semicond. Sci. Technol. **26** (2011) 095018 (5pp) doi:10.1088/0268-1242/26/9/095018

Electrical properties of stacking electrodes for flexible crystalline semiconductor photonic devices

Weiquan Yang[1], Rui Li[1,2], Zhenqiang Ma[3] and Weidong Zhou[1]

[1] NanoFAB Center, Department of Electrical Engineering, University of Texas at Arlington, Arlington, TX 76019, USA
[2] Institute of Near-field Optics and Nano Technology, School of Physics and Optoelectronic Technology, Dalian University of Technology, Dalian 116024, People's Republic of China
[3] Department of Electrical and Computer Engineering, University of Wisconsin-Madison, WI 53706, USA

E-mail: wzhou@uta.edu

Received 12 April 2011, in final form 9 July 2011
Published 3 August 2011
Online at stacks.iop.org/SST/26/095018

Abstract
We report here electrical properties of low-temperature-stacked electrodes for large-area flexible photonic devices, based on single-crystalline InP nanomembrane (NM) transfer and stacking processes. Au, Al and ITO electrodes were investigated. An excellent ohmic contact was demonstrated on the stacked InP NM–ITO electrode, with a measured contact resistivity of 0.45 Ω cm^2. Two types of flexible InP solar cells were also fabricated and characterized, based on the stacked InP NM–ITO and InP NM–Al contacts, respectively. The efficiency of solar cells with ITO as back contact is five times higher than that with Al as back contact. Such low-temperature energy-efficient NM transfer and electrode-stacking techniques can be applied to a wide range of flexible thin film photonic devices.

(Some figures in this article are in colour only in the electronic version)

1. Introduction

Flexible electronic and photonic structures, the properties of which can be expanded and manipulated for electronic and photonic device applications via mechanical bending, are of great scientific and engineering importance. Such devices have their applications ranging from flexible imaging/displays, sensors, solar cells and conformal electronic/photonic integrated systems to potential integration into artificial muscles or biological tissues. Most flexible electronics research so far is based on organic, polymer and/or amorphous semiconductor material systems [1–4]. On the other hand, higher performance flexible devices can be realized based on much higher quality flexible crystalline semiconductor nanomembranes (NMs). The high-quality single-crystalline silicon NMs (Si NM) have been released and transferred onto various foreign substrates, such as glass, flexible PET (polyethylene terephthalate) plastics, etc, based on low-temperature transfer and stacking processes [5–10]. Very high performance electronics based on transferable Si/SiGe NMs were already reported. NMs based on III–V (GaAs, InP, etc) and other material systems are also being developed for heterogeneous integration (membrane stacking) on Si and other foreign substrates, with desired electronic and photonic functions [11–16].

Unlike rigid-substrate-based devices, for which heavy doping of semiconductors and thermal annealing of the contacts can be conventionally used for forming ohmic contacts, it is quite challenging to form ohmic contacts on NMs transferred to low-temperature plastic substrates. Recently, we formed ohmic contacts on transferrable SiNMs by pre-doping them before release [17]. Those metal ohmic contacts were formed by conventional e-beam evaporation of metal on SiNMs. For plastic substrate-based flexible electronics and optoelectronic devices, such as solar cells, reduced thermal budget and simpler fabrication process are needed. Forming high-quality ohmic contacts without involving a vacuum-based process or a thermal process is thus highly desired. However,

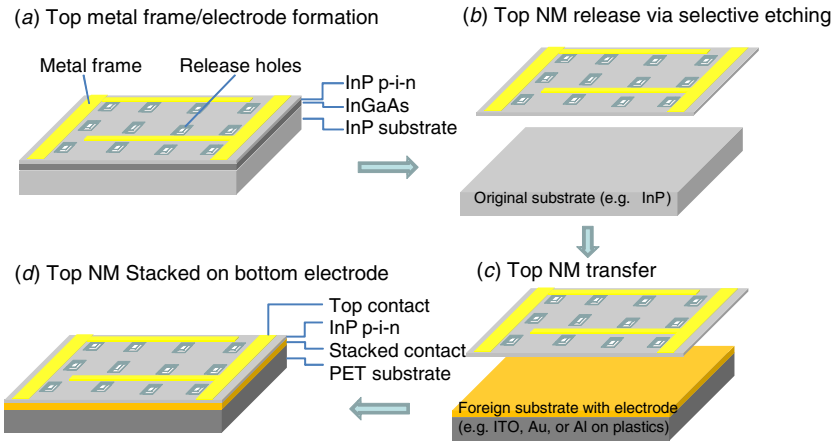

Figure 1. Room temperature energy-efficient NM transfer and electrode-stacking process. (*a*) Formation of release holes and top metal frames on the top InP NM layer for frame-assisted membrane transfer; (*b*) top InP NM release via selective wet etching of the sacrificial layer (e.g. InGaAs here), (*c*) top NM transfer onto the foreign substrate with the electrode (e.g. ITO-coated flexible plastic substrate); and (*d*) final device with the stacked bottom InP NM–ITO electrode.

such a process has not been demonstrated. Here we report high-quality ohmic contacts that were formed without using any annealing or vacuum environment. We directly stack and bond highly doped semiconductor (InP) NM with Al, Au and ITO, and characterize the electrical properties of the annealing-free-stacked semiconductor NM-electrode configurations. We found that high-quality ohmic contacts can be formed between the InP NM and ITO. Based on such stacked electrodes, large-area flexible solar cells have been demonstrated, based on transferred crystalline InP NMs.

2. Experiments

The low (room) temperature energy-efficient NM transfer and electrode-stacking process is shown schematically in figure 1. The starting material is a p-i-n InP layer (total thickness of 1 μm) grown on top of an InP substrate, with an InGaAs sacrificial layer sandwiched in between. Due to the weak mechanical properties of InP, it is a significant challenge to transfer larger area InP NMs without using any other supporting structures. We reported earlier a metal-frame-assisted membrane transfer (FAMT) process for this purpose [16]. The Au finger contact (80 nm) here was formed on top of InP NM to offer desired mechanical strength for the successful transfer of large area InP NMs (figure 1(*a*)). For solar cell devices, this Au finger contact also serves as top electrode contact. Then release holes were formed on the top InP layer using wet etching. After etching away the sacrificial InGaAs layer, the metal-framed InP layer is detached from the InP-based substrate (figure 1(*b*)). The PET substrate with processed electrodes is used to pick up the InP NM. A final structure with a top metal-frame electrode and a bottom-stacked InP NM–ITO electrode is shown in figure 1(*d*). Note here that the bottom contact is formed by stacking the highly doped InP NM layer on an electrode layer (ITO, Al or Au) at room temperature. Here no high-temperature annealing processes are involved. The FAMT process is highly repeatable, and we get a high yield of almost 80% for the successful transfer.

Shown in figure 2 are fabricated and transferred device structures. The thicknesses of p-, i- and n-type InP layers are 400, 100 and 500 nm, respectively (figure 2(*a*)). A microscope image of a large-area InP NM transferred to the flexible PET substrate is shown in figure 2(*b*). The size of the transferred InP NM is 3 mm $\times$ 3 mm. The distance between two adjacent framed metal fingers is 200 μm. Note that the size of the transferred membranes reported here is limited by the size of the designed patterns on the mask. Much larger NMs can be transferred. It is also worth noting that the processes reported here can also be applied to other types of semiconductor materials, including Si, GaAs, etc.

Transfer length method (TLM) measurements [18] were employed to characterize the contact resistance of the stacked InP NM–ITO contacts. PET plastic sheets with different thin film coatings (i.e., ITO, Al, Au) were used as substrates. Patterned ITO electrodes were formed by wet etching using the HCl and H_3PO_4 solution (1:4). Patterned Al or Au contacts were also formed, as reference samples, by thermal evaporation and wet etching processes. InP NMs were transferred to the patterned electrodes on PET substrates with different back contacts. The schematic structures and microscope image of InP NM transferred to the patterned ITO contacts on flexible PET substrates is shown in figure 2(*c*). The distances between two adjacent ITO electrodes are 50, 100, 150, 200, 250, 300 μm, respectively. The width of each electrode is 100 μm. The width of the InP NM is 3 mm. Figure 2(*d*) shows the image of the flexible InP NM on PET substrates under the bending status.

3. Results and discussion

Measured current–voltage (*I–V*) characteristics of the InP NM stacked on bottom ITO, Al and Au electrodes at room temperature are shown in figure 3. The distance between the two electrodes for all three samples is 50 μm. The nearly linear behavior of the *I–V* curve for the InP NM stacked on ITO electrodes shows that the ohmic contact was formed between the InP NM and the back ITO electrode, with very low contact

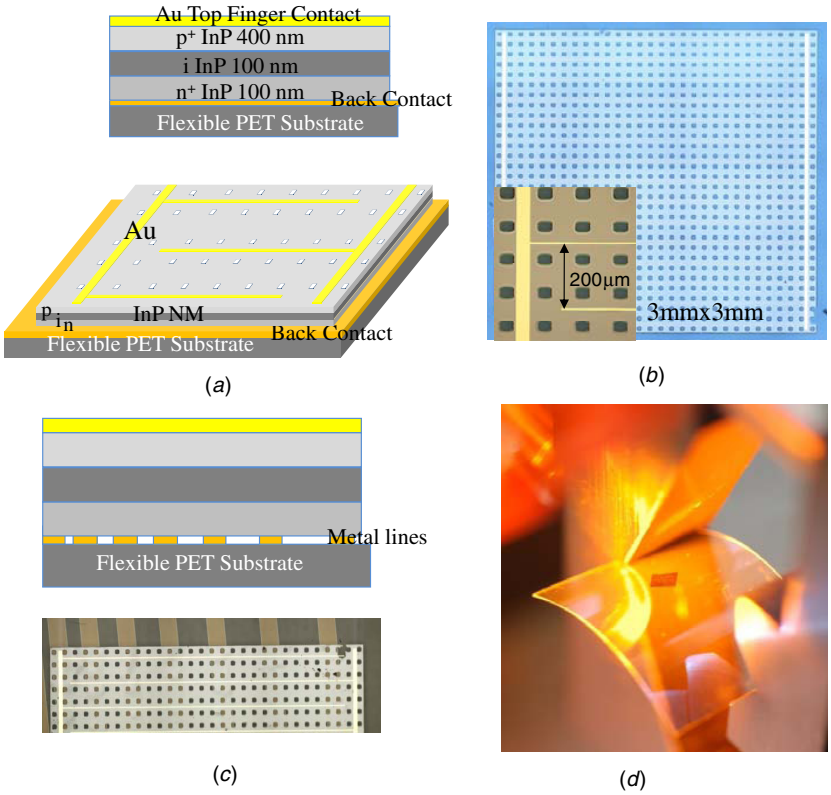

Figure 2. (*a*) Schematics of a vertical InP p-i-n nanomembrane (NM) transferred onto flexible PET substrates based on the frame-assisted transfer process; (*b*) a microscope image of the InP NM transferred onto PET substrates, and zoom-in pictures shown in the inset; (*c*) cross-section schematics and microscope image of the vertical InP p-i-n NM transferred onto multi-electrodes with different distances on PET substrates; and (*d*) a close-up image of the bended flexible InP NM on the PET substrate.

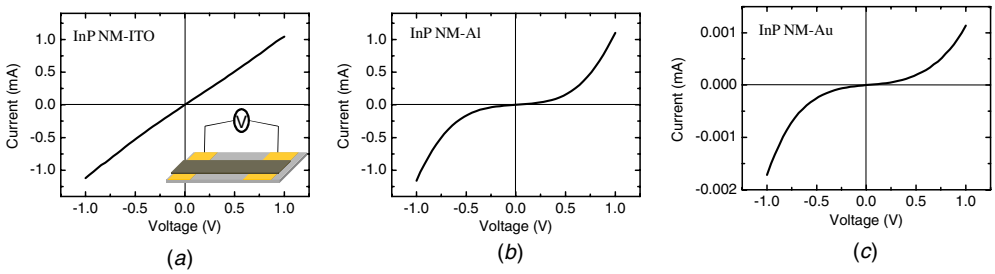

Figure 3. Measured two-probe *I*–*V* curve of InP NM stacking onto: (*a*) ITO, (*b*) Al, and (*c*) Au.

resistance. On the other hand, the symmetric nonlinear *I*–*V* curve for the InP NM stacked on Al, or Au electrodes indicates very large contact resistance. In other words, ohmic contacts were not formed. For these contacts, significant potential barriers exist at the contact interfaces partially blocking the current flow. Under the same bias voltage (1 V), the current flow for the InP NM–Au contact structure is three orders smaller than that of the ITO contact. The difference of current levels between the Al contact and the Au contact may be related to different work functions of Au and Al. The work function of Au is higher than that of Al.

The TLM measurement is used to characterize the contact resistance of InP NM metal. A test structure makes use of multiple contacts along the length of the InP NM, as shown in figure 4(*a*). We can extract the contact resistance R_c by the TLM measurement according to the following equation [18]:

$$R = 2R_c + \rho \times L/S,$$

where ρ is the resistivity of the InP NM, L is the transmission length, S is the area of cross-section of the InP NM. The *I*–*V* curves between two adjacent electrodes with a different distance are shown in figure 4(*b*). Under the same bias conditions, the current decreases linearly with the increase of the electrode distance. Figure 4(*c*) shows the total resistance obtained from the *I*–*V* characteristics as a function of the length between two adjacent metal contacts. R_c can be extracted from the intersection of the linear fit at the axis of the total resistance. The difference between the fitted value resistance and experimental data may be related to the different adhesion conditions between the InP NM and different back electrodes. The specific contact resistivity ρ_c is defined as $\rho_c = R_c \times A$,

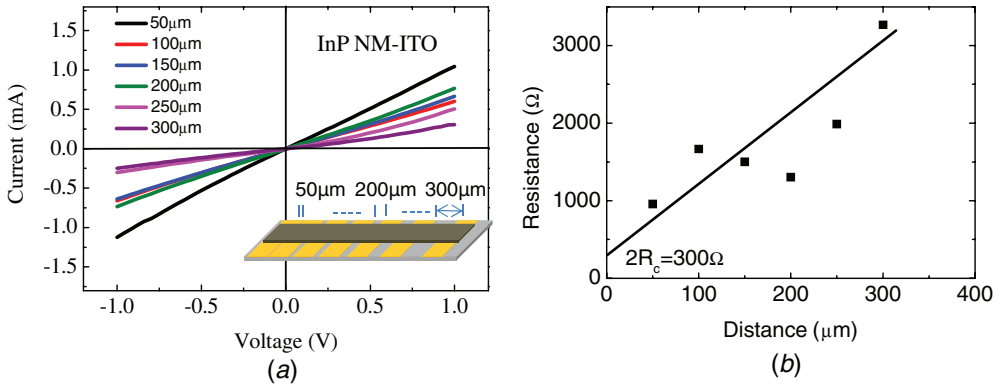

Figure 4. (*a*) Current–voltage curves of InP NM–ITO with different distance and (*b*) the measured total resistance of stacked InP NM–ITO.

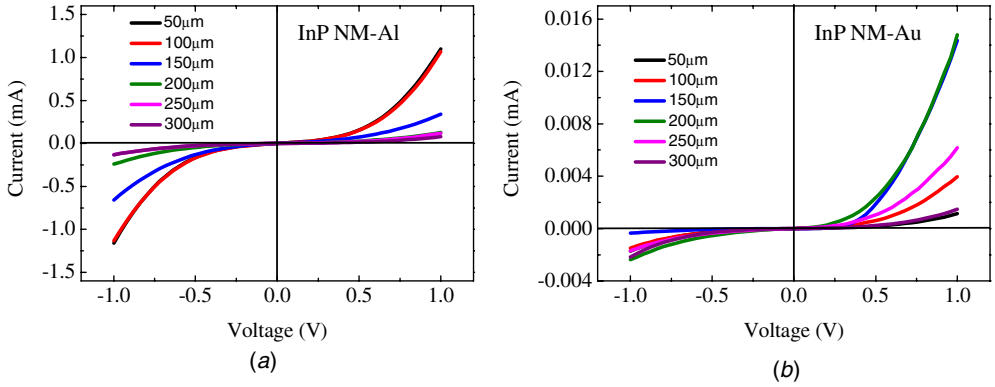

Figure 5. Current–voltage curves of (*a*) InP NM–Al and (*b*) InP NM–Au with different distances.

where A is the contact area. Consequently, the specific contact resistivity of 0.45 Ω cm^2 was determined experimentally from the TLM measurement. The transfer length measurements of InP NM–Al and InP NM–Au contacts were also carried out to further examine the contact properties. The characterization results are shown in figures 5(*a*) and (*b*), respectively. With different distances between the back contact electrodes, we obtained nonlinear current–voltage curves, which is similar to the results shown in figure 3. Such nonlinear properties at any distance between the two back contact electrodes further confirm that the stacked InP NM–Al and InP NM–Au do not form good ohmic contacts (with large contact resistance and/or rectifying effect, which is due to the potential barriers at the interfaces).

In order to evaluate the effects of contacts on device performance, we fabricated InP NM solar cells, with stacked InP NM–ITO back contact. A reference cell with stacked InP NM–Al contact was also processed. The fabrication process is shown in figure 1, where top Au electrodes were formed by e-beam evaporation before InP NM transfer and bottom InP NM–ITO electrodes were formed by stacking after transfer. All processes were carried out at room temperature.

The performance characteristics of the solar cells are shown in figure 6. For InP solar cells with ITO back contact, we obtained photovoltaic solar cells with an open circuit voltage of 0.64 V, a short circuit current of 0.59 mA and a power efficiency of 1%. For InP solar cells with Al back contact, the open circuit voltage, short circuit current and power efficiency are 0.66 V, 0.22 and 0.2%, respectively. The

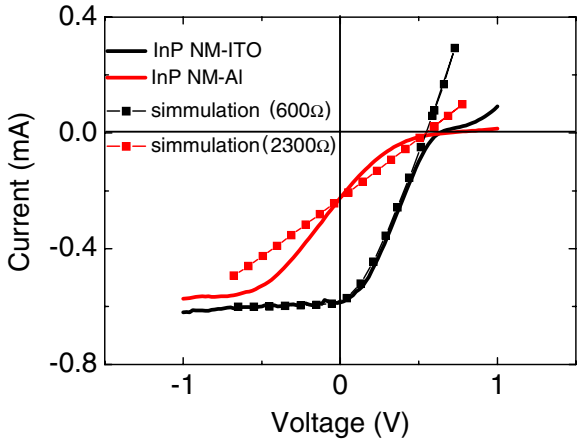

Figure 6. Measured characteristics of the flexible crystalline InP thin film solar cell stacked on ITO and Al back contact; the simulated *I–V* curve of the InP solar cell with different series resistance, under standard AM solar simulator test conditions at room temperature.

efficiency for the solar cells with ITO as the back contact is five times larger than that with Al contact. This is mainly due to the better ohmic contact of the InP NM with ITO and with Al. PC1D [19] was used to simulate the performance of these two types of solar cells. The modeled *I–V* curve with a series resistance of 600 Ω matches with that of the InP NM–ITO solar cell. The other one with a series resistance of 2300 Ω matches with that of the InP NM–Al solar cell. The simulations indicate that the series resistance is much smaller

for the InP NM–ITO solar cell than that for the InP NM–Al solar cell, which further confirms excellent ohmic contact formation for the stacked InP NM–ITO contact. Note that the solar cell reported here can have much high efficiency, with proper surface texturing/anti-reflection coating, and optimized electrical/optical configurations [20, 21].

4. Conclusions

The InP p-i-n NM was stacked onto multi-electrodes on flexible PET substrates using a frame supported transferring process. The electrical properties of stacked contacts between the InP NM and different electrode (ITO, Al and Au) were investigated. The stacked InP NM–ITO contact has excellent ohmic contact characteristics, with the measured contact resistance of 0.45 Ω cm^2. A flexible InP solar cell stacking on back ITO and Al contact was fabricated and characterized to check the contact property further. The efficiency of the solar cell with back ITO contact is 1%, which is much higher than that with back Al contact. The study indicates a route toward high-performance optoelectronic devices with reduced processing procedures and lower cost.

Acknowledgments

This work is supported in part by US AFOSR MURI program under grant FA9550-08-1-0337, and in part by US ARO (W911NF-09-1-0505). RL acknowledges CSC scholarship funding for financial support.

References

[1] Park J W, Shin D C and Park S H 2011 Large-area OLED lightings and their applications *Semicond. Sci. Technol.* **26** 034002
[2] Li F M, Nathan A, Wu Y L and Ong B S 2007 *Appl. Phys. Lett.* **90** 133514
[3] McGarry S P and Tarr N G 2008 *Semicond. Sci. Technol.* **23** 055009
[4] Ng T N, Lujan R A, Sambandan S, Street R A, Limb S and Wong W S 2007 *Appl. Phys. Lett.* **91** 063505
[5] Ahn J, Kim H, Lee K, Jeon S, Kang S, Sun Y, Nuzzo R and Rogers J 2006 *Science* **314** 1754
[6] Sun L, Qin G, Celler G K, Zhou W and Ma Z 2010 *Small* **6** 2553–7
[7] Scott S A and Lagally M G 2007 *J. Phys. D: Appl. Phys.* **40** R75–92
[8] Zhou W, Ma Z, Yang H, Qiang Z, Qin G, Pang H, Chen L, Yang W, Chuwongin S and Zhao D 2009 *J. Phys. D: Appl. Phys.* **42** 234007–17
[9] Yuan H C, Ma Z, Roberts M M, Savage D E and Lagally M G 2006 *J. Appl. Phys.* **100** 013708
[10] Rogers J, Someya T and Huang Y 2010 *Science* **327** 1603
[11] Sun Y G, Kumar V, Adesida I and Rogers J A 2006 *Adv. Mater.* **18** 2857
[12] Sysak M N, Anthes J O, Bowers J E, Raday O and Jones R 2008 *Opt. Express* **16** 12478–86
[13] Yang W Q, Yang H J, Qin G X, Ma Z Q, Berggren J, Hammar M, Soref R and Zhou W D 2010 *Appl. Phys. Lett.* **96** 121107
[14] Yoon J, Jo S, Chun I S, Jung I, Kim H S, Meitl M, Menard E, Li X L, Coleman J J, Paik U and Rogers J A 2010 *Nature* **465** 329–33
[15] Yang W, Yang H, Qin G, Pang H, Berggren J, Hammar M, Soref R, Ma Z and Zhou W 2009 Crystalline silicon nanomembrane stacking for large-area flexible photodetectors *6th Int. Conf. on Group IV Photonics (San Francisco, CA)* 110–2
[16] Yang W, Yang H, Qin G, Ma Z, Berggren J, Hammar M, Soref R and Zhou W 2010 *Appl. Phys. Lett.* **96** 121107
[17] Yuan H C and Ma Z 2006 *Appl. Phys. Lett.* **89** 212105
[18] Schroder D K 2006 *Semiconductor Material and Device Characterization* (New York: Wiley-Interscience)
[19] Basore P A 1990 *IEEE Trans. Electron. Dev.* **37** 337–43
[20] Bergmann R 1999 *Appl. Phys.* A **69** 187–94
[21] Zhou W, Tao M, Chen L and Yang H 2007 *J. Appl. Phys.* **102** 103105